

CUSUM AND EWMA MULTI-CHARTS FOR DETECTING A RANGE OF MEAN SHIFTS

Dong Han¹, Fugee Tsung², Xijian Hu³ and Kaibo Wang²

¹*Shanghai Jiao Tong University*

²*Hong Kong University of Science and Technology and*

³*Xinjiang University*

Abstract: The multi-chart consists of several CUSUM or EWMA charts with different reference values that are used simultaneously to detect anticipated process changes. We not only prove that the chart can quickly achieve the asymptotic optimal bound, but also give an integral equation to determine the reference values to arrive at optimality. Simulation results are used to verify the theoretical optimal properties and to show that the CUSUM multi-chart is superior on the whole to single CUSUM, single EWMA, and EWMA multi-charts in terms of run length and robustness, and can compete with GLR control charts in detecting a range of various mean shifts. We investigate the design of both CUSUM and EWMA multi-charts. Some practical guidelines are provided for determining multi-chart parameters, such as the number of constituent charts and the allocation of their reference values.

Key words and phrases: average run length, change point detection, statistical process control.

1. Introduction

Statistical process control (SPC) techniques are widely used in monitoring and controlling both manufacturing and service processes. Various SPC schemes have been extensively studied in the literature, among them the cumulative sum (CUSUM) and exponential weighted moving average (EWMA) schemes (see Montgomery (1996), Lai (1995), and references therein). The performance of these schemes, however, mostly depends on the pre-specified size of the shifts in the variables that one wishes to detect. For example, it has been shown by Moustakides (1986) and Ritov (1990) that the performance in detecting the mean shift of the one-sided CUSUM control chart with the reference value δ is optimal in terms of average run length (ARL) if the actual mean shift is δ . Srivastava and Wu (1993, 1997) and Wu (1994) provided a design of the optimal EWMA by choosing an optimal weighting parameter in an EWMA control chart such that it can minimize the out of control ARL for a given reference value, and

they illustrated that the optimal EWMA performs almost as well as the CUSUM chart in terms of ARL. Lucas and Saccucci (1990) also provided the optimal design parameters of an EWMA chart that depends on a pre-specified size of mean shift as well as a given in-control ARL.

Some schemes do not depend on a specific shift size δ , for example the GLR chart of Siegmund and Venkatraman (1995). Their simulation results show that the GLR chart is better than the CUSUM control chart in detecting a mean shift that is larger or smaller than δ , and is only slightly inferior in detecting a mean shift of size δ . Also, by taking the maximum weighting parameter in the EWMA control chart, Han and Tsung (2004) proposed a generalized EWMA (GEWMA) control chart that does not depend on the reference value, and proved that the GEWMA control chart is better than the optimal EWMA in detecting a mean shift of any size when the in-control ARL is large. However, these methods usually require complex computing and have not been regularly applied to real on-line problems.

Because we rarely know the exact shift value of a process before it is detected, it may be more important to look at a range of known or unknown mean shifts. Examples include a semiconductor wafer manufacturing process that needs to monitor and detect a range of anticipated changes in the position and size of serial markings, and a wire manufacturing process that requires continuous diameter monitoring using laser micrometers for a wide range of unknown shifts.

To handle this problem, an alternative approach is to consider a multiple model or a mixture of several control charts. In fact, Lorden (1971) has already considered and studied such a model. Since then, Lorden and Eisenberger (1973), Lucas (1982), Rowlands et al. (1982), Dragalin (1993, 1997) and Sparks (2000) have further investigated and studied a combination of several CUSUM charts and a combined Shewhart-CUSUM to detect mean shifts in a range. They have shown the efficiency of the combined CUSUM and Shewhart-CUSUM charts, and provided various designs for these procedures, based on numerical simulations.

The combination of several CUSUM charts mentioned above can be called CUSUM multi-chart, to consist of multiple CUSUM charts with different reference values that are used simultaneously to detect the mean shift. For example, let the anticipated interval of the mean shift, μ , be $[a, b]$. Then, we can create a CUSUM multi-chart with a number of CUSUM charts, $T_C(\delta_1), \dots, T_C(\delta_m)$ (see (2.1) in Section 2 for the definition of $T_c(\delta_1)$), by choosing the parameter values, $\delta_1, \dots, \delta_m$, in the interval. If one of the CUSUM charts, $T_C(\delta_k)$, triggers a signal of having a mean shift, the multi-chart would send an out-of-control warning. The CUSUM multi-chart has its roots in conventional control charts and has much reduced computational complexity compared with GLR and GEWMA. Although the reference δ can be defined in a more general sense (e.g., a dynamic,

non-constant mean change) in using the multi-chart, we focus on the cases with constant mean shifts at first. Also, the constituent charts of the multi-chart have great flexibility in taking various forms of charts, but in the paper we mainly investigate the CUSUM and EWMA multi-chart.

Although the general theoretical results regarding asymptotic optimality have been given by Lorden (1971), it is not clear whether the CUSUM multi-chart has some special asymptotic optimal properties. Although Rowlands et al. (1982) and Sparks (2000) have shown that two or three CUSUMs were sufficient to almost achieve the optimal envelope, it is not clear whether there exists an optimal design of the CUSUM multi-chart that can be carried out by theoretical calculation and Monte Carlo simulation. The primary goal of this paper is to deal with these two problems. It will be shown that the CUSUM multi-chart cannot only quickly achieve the asymptotically optimal bound but also has better performance (quicker and more robust) than that of a single CUSUM and EWMA control charts in detecting a range of various mean shifts. An optimal design of the CUSUM multi-chart is provided for determining the multi-chart parameters, such as the number of constituent charts and the allocation of their reference values.

The remainder of the paper is organized as follows. In the next section, we discuss some properties related to the CUSUM multi-chart, EWMA multi-chart and GLR chart. A novel charting performance index is proposed in Section 3 for the situation with a range of known or unknown shifts. Based on that, the performances of the CUSUM multi-chart and the EWMA multi-chart are compared with their constituent charts and the GLR chart in Section 4. Also in that section, the fast asymptotic optimality of the CUSUM multi-chart and the integral equation to determine the optimal choice of the reference values are presented. Section 5 provides an optimal design of the CUSUM multi-chart and some practical guidelines for both CUSUM multi-charts and EWMA multi-charts to determine the number of constituent charts and allocation of their reference values. Conclusions and problems for further study are discussed in Section 5, with the proofs of three theorems given in the Appendix.

2. The CUSUM and EWMA Multi-Charts

Let X_i , $i = 1, \dots$, be $N(\mu_0, \sigma)$. Suppose that at some time period τ , usually called a change point, the probability distribution of X_i changes from $N(\mu_0, \sigma)$ to $N(\mu, \sigma)$. In other words, from time period τ onwards, X_i has the common distribution $N(\mu, \sigma)$. Thus, the mean of X_i undergoes a persistent shift of size $\mu - \mu_0$, where μ_0 and σ are known and, without loss of generality, assumed to be $\mu_0 = 0$ and $\sigma = 1$.

Let $\Delta_m = \{\delta_k : 1 \leq k \leq m\}$ and $R_m = \{r_k : 1 \leq k \leq m\}$ be two sets of numbers, where $\delta_k > 0$ and $0 < r_k \leq 1$ are known reference values. Let $c_k > 0$ and $d_k > 0$ be two numbers that usually depend on δ_k and r_k , respectively. Then the one-sided CUSUM and EWMA multi-charts, $T_C^*(\Delta_m, C_m)$ and $T_E^*(R_m, D_m)$, are $T_C^* = \min_{\delta_i \in \Delta_m} \{T_C(\delta_i, c_i)\}$ and $T_E^*(R_m, D_m) = \min_{r_i \in R_m} \{T_E(r_i, d_i)\}$ where

$$T_C(\delta_i, c_i) = \min\{n : \max_{1 \leq k \leq n} \delta_i [X_n + \cdots + X_{n-k+1} - \delta_i k/2] > c_i\}, \quad (2.1)$$

$$T_E(r_i, d_i) = \min\{n : \sum_{k=0}^{n-1} r_i (1 - r_i)^k X_{n-k} > d_i\}. \quad (2.2)$$

Here, $T_C(\delta_i, c_i)$ and $T_E(r_i, d_i)$ are, respectively the one-sided CUSUM and EWMA charts. As can be seen, for the observations X_1, \dots, X_n , one requires mn calculations for the CUSUM multi-chart to detect a mean shift. The GLR and GEWMA charts (see Siegmund and Venkatraman (1995) and Han and Tsung (2004)) are $T_{GL}(c) = \min\{n : \max_{1 \leq k \leq n} |[X_n + \cdots + X_{n-k+1}]/k^{1/2}| > c\}$ and $T_{GE}(c) = \inf\{n \geq 1 : \max_{1 \leq k \leq n} |\bar{W}_n(\frac{1}{k})| \geq c\}$, where

$$\bar{W}_n\left(\frac{1}{k}\right) = \frac{\sqrt{(2 - \frac{1}{k})}}{\sqrt{\frac{1}{k}[1 - (1 - \frac{1}{k})^{2n}]}} \sum_{i=0}^{n-1} \frac{1}{k} (1 - \frac{1}{k})^i X_{n-i},$$

and require $n(n+1)/2$ calculation. In particular, when n is large, e.g., 1,000, the computational burden for the GLR chart is very heavy. Thus, the multi-chart has an advantage in reducing computational complexity compared with the GLR and GEWMA charts.

In addition to its computational advantage, we will demonstrate its performance in detecting a wide range of anticipated changes, and its flexibility in design for various situations.

3. Charting Performance Index for a Range of Mean Shifts

The average run length (ARL) has been extensively used in evaluating different charting methods. For comparison, the in-control ARL (ARL_0) of all candidate charts are forced to be equal, and to correspond to the same level of type I error. The chart that has the lowest out-of-control ARL at the desired mean shift size presents the highest power to detect the pre-specified shift.

Although the ARL is a popular criterion, it has a deficiency in evaluating a charting performance for a range of anticipated mean shifts. For example, Figure 1 shows the ARL curves of two CUSUM charts, one designed for detecting a mean shift size of 0.1, the other of 2.0. The ARL curves intersect at a mean shift of about 0.77. Thus, the chart designed for 0.1 outperforms the chart for 2.0 in

the range of $(0, 0.77)$, while the chart for 2.0 outperforms the chart for 0.1 in the range of $(0.77, 4.0]$. It would be difficult to evaluate their performance if the whole range of mean shifts is of interest.

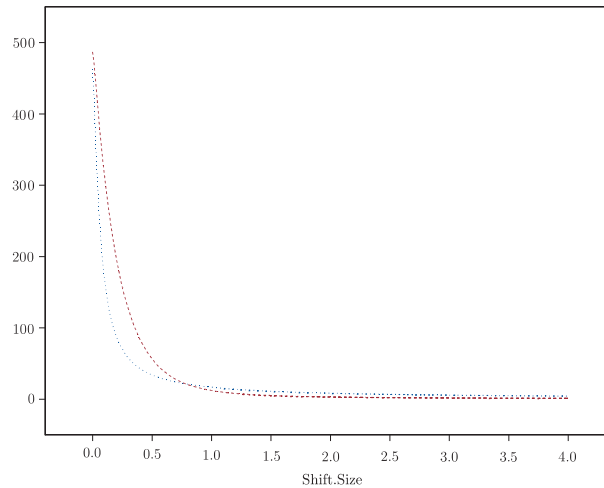


Figure 1. ARL curves of two CUSUM charts designed for mean shifts of 0.1 and 2.0.

To handle such a situation, we propose an Overall Charting Performance Index (OCPI) as follows.

$$OCPI_{uf} \left(\int_a^b w(\mu) \frac{ARL(\mu) - ARL_r(\mu)}{ARL_r(\mu)} d\mu \right), \quad (3.1)$$

where $\mu \subset [a, b]$ is a shift size in the anticipated range within which the performance is evaluated, $ARL(\mu)$ is the ARL of the chart to be evaluated, and $ARL_r(\mu)$ is a reference or baseline with the lowest ARL value at the shift size μ . It is known that the CUSUM chart with the parameter δ achieves the lowest ARL at the shift $\mu = \delta$ among all CUSUM schemes, so that the ARL value at each shift size μ within the range $[a, b]$ will be used as a lower bound ARL_r in our later study. The reference curve that is a composite of a collection of the lowest possible ARL at each shift size is denoted as an Optimal ARL Curve (OAC).

Note that $w(\mu)$ is a weighting function to emphasize various mean shifts within a range based on prior knowledge and experience with the process, given preferential consideration to certain mean shifts. For example, if the "large" mean shift (e.g., $\mu \geq 2$) is considered to be more important than the "small" one (e.g., $\mu < 2$), this can be acknowledged. Thus, we can compare the performance of charts by the OCPI to know which is better in detecting "large" mean shifts. If no

prior information or preference is provided, we use $w(\mu) = (b - a)^{-1}$ throughout the range.

As can be seen, the range of OCPI values is from 0 to $+\infty$. If we choose $f(x) = e^{-x}$, the range of the OCPI is $(0, 1]$. In addition, the OCPI with $f(x) = e^{-x}$ is more communicable and comparable by denoting "0" as the worst detection performance and "1" as the best performance for a chart. Moreover, the comparison results do not change as long as the selected functions are all strictly monotonic decreasing (or increasing). Here we take $f(x) = e^{-x}$.

If the specific sizes of the anticipated mean shifts within a range are known, we modify the OCPI in (4.1) to the following form:

$$OCPI_k = f\left(\sum_{i=1}^n w_i \frac{ARL_i - ARL_{ri}}{ARL_{ri}}\right), \quad (3.2)$$

where $i = 1$ to n represents the n sizes of anticipated mean shifts, and $w_i = 1/n$.

4. Asymptotic Analysis of the CUSUM Multi-Chart

The CUSUM chart is popular and has attractive theoretical properties in that it is the optimal test for a known mean shift, but it does less well for a range of shifts away from its designed shift (see Hawkins and Olwell (1998)). The GLR chart, on the other hand, is good for unknown mean shifts. However, it is less popular due to its excessive computational effort. In this section, we start with the investigation of the CUSUM multi-chart by proving its asymptotic optimality in detecting a range of known and unknown mean shifts, and then compare the detection performance of the CUSUM multi-chart and the EWMA multi-chart with their constituent CUSUM charts, EWMA charts, and GLR charts.

4.1. The anticipated mean shifts, μ_k , are known

Here, we suppose anticipated mean shift sizes, $\mu_k (1 \leq k \leq n)$, in a range are known from prior knowledge and experience.

For a stopping time, T , as the alarm time in a detecting procedure, we have the in-control $ARL_0(T) = E_0(T)$, and the out-of-control $ARL_\mu(T) = E_\mu(T)$. Let $T(\mu_k, c_k)$ and $T(\mu_k, c'_k)$ be two one-sided CUSUM charts with different control limits c_k and c'_k . Denote $T(\mu_k, c_k)$ and $T(\mu_k, c'_k)$, respectively, as T_k and T'_k . Consider the CUSUM multi-chart $T_C^* = \min_{1 \leq k \leq n} \{T'_k\}$. Take the control limits, c'_1, \dots, c'_n , such that $c'_k > c_k$, $1 \leq k \leq n$, and

$$\begin{aligned} E_0(T'_1) &= \dots = E_0(T'_n) = L' \\ &> E_0(T_1) = \dots = E_0(T_n) = L = E_0(T_C^*). \end{aligned} \quad (4.1)$$

This means that the CUSUM charts, T_1, \dots, T_n and the CUSUM multi-chart, T_C^* , have a common ARL_0 , i.e., $E_0(\cdot) = L$. It has been shown by Lorden (1971), Moustakides (1986), Srivastava and Wu (1997) and Wu (1994), that the CUSUM chart, T_k , is optimal and the optimal lower boundary is $2 \log L / \mu_k^2 + \text{Constant}$. That is, for an arbitrary control chart T subject to the constraint $E_0(T) \geq L$, $E_{\mu_k}(T) \geq E_{\mu_k}(T_k)$ holds for $1 \leq k \leq n$ and

$$E_{\mu_k}(T_k) = \frac{2 \log L}{\mu_k^2} + M(\mu_k) + o(1)$$

for $1 \leq k \leq n$ as $L \rightarrow \infty$, where $M(\mu_k) = -2/\mu_k^2 + 2\mu_k^{-2} \ln(\mu_k^2/2)$ and $o(1) = O(L^{-1} \ln(\mu^2 L/2))$. Thus, the expectation of the optimal lower boundaries can be written as

$$B(L) = \sum_{k=1}^n P(Z = \mu_k) \left(\frac{2 \log L}{\mu_k^2} + M(\mu_k) \right),$$

where $P(Z = \mu_k)$ denotes the probability that the mean shift size Z is μ_k and $\sum_{k=1}^n P(Z = \mu_k) = 1$. Asymptotic optimality of the CUSUM multi-chart rescue from the following theorem.

Theorem 1. *Let $P(Z = \mu_k) = \pi_k$ for $1 \leq k \leq n$. As $L \rightarrow \infty$, or $\min_{1 \leq i \leq n} \{c_i\} \rightarrow \infty$, we have $\log L' - \log L \rightarrow 0$ and*

$$\left| \sum_{k=1}^n \pi_k E_{\mu_k}(T_C^*) - B(L) \right| \leq O\left(\frac{(\ln L)^3}{L}\right) = O(c_1^3 e^{-c_1}) \rightarrow 0. \tag{4.2}$$

Remark 1. Let $L' = nL$, that is, each CUSUM chart T'_k ($1 \leq k \leq n$) has the same in-control $ARL_0 = nL$ for some large L . Note that $T_C^* \leq T'_k$ for $1 \leq k \leq n$. It follows from Theorem 1 of Lorden (1971), in conjunction with Lorden's remark following his Theorem 2, that the CUSUM multi-chart has in-control $ARL_0 \geq L$ and

$$\begin{aligned} \frac{2 \log m + 2 \log L}{\mu_k^2} + M(\mu_k) + o(1) &= E_{\mu_k}(T'_k) \geq E_{\mu_k}(T_C^*) \geq E_{\mu_k}(T_k) \\ &= \frac{2 \log L}{\mu_k^2} + M(\mu_k) + o(1) \end{aligned}$$

for $1 \leq k \leq n$ as $L \rightarrow \infty$. That is,

$$2 \log m \sum_{k=1}^n \frac{\pi_k}{\mu_k^2} + o(1) \geq \sum_{k=1}^n \pi_k E_{\mu_k}(T_C^*) - B(L) \geq o(1)$$

as $L \rightarrow \infty$, so (4.2) can not be deduced directly from Theorem 1 of Lorden (1971).

The proof of Theorem 1 is given in the appendix.

Corollary 1. *If a control chart, T , is subject to the constraint $E_0(T) \geq L$ and $E_{\mu_k}(T) \geq \bar{E}_{\mu_k}(T), 1 \leq k \leq n$, then*

$$\sum_{k=1}^n \pi_k E_{\mu_k}(T) \geq \sum_{k=1}^n \pi_k E_{\mu_k}(T_C^*) \tag{4.3}$$

as $L \rightarrow \infty$, where $\bar{E}_{\mu}(T) = \sup_{\tau \geq 1} \text{ess sup } E_{\mu}[(T - \tau + 1)^+ | X_1, \dots, X_{\tau-1}]$, τ is change time (see Lorden (1971)). Specifically, for each CUSUM chart T_j satisfying (4.1) ($1 \leq j \leq n$) and $n > 1$, we have, as $L \rightarrow \infty$,

$$\sum_{k=1}^n \pi_k E_{\mu_k}(T_j) \geq \sum_{k=1}^n \pi_k E_{\mu_k}(T_C^*). \tag{4.4}$$

It follows from (4.4) that the CUSUM multi-chart performs better than any single CUSUM chart in detecting more than one anticipated mean shift when $L = ARR_0 \rightarrow \infty$. This property will be seen later in Monte Carlo simulations.

4.2. The anticipated mean shift, μ , is unknown

Now we investigate the situation where we know the anticipated range to monitor but the specific size of an anticipated mean shift is unknown.

Let $a > 0$. Here we choose the reference values δ_k in $[a, b]$ such that $a \leq \delta_k < \delta_{k+1} \leq b$ for $0 \leq k \leq m$, where $\delta_0 = 0$ and $\delta_{m+1} = b$. Let $I_k = \{\mu : (\delta_{k-1} + \delta_k)/2 < \mu \leq (\delta_k + \delta_{k+1})/2\}$ for $1 \leq k \leq m$. Denote by $OCPI_u(\delta_1, \dots, \delta_m)$ the OCPI of the CUSUM multi-chart, $T_C^* = \min_{1 \leq k \leq m} \{T'_k\}$, where $T'_k = T(\delta_k, c'_k)$ is the CUSUM chart with the reference value δ_k ($1 \leq k \leq m$) satisfying (4.1). Here we take $w(\mu) = (b - a)^{-1}$ and $f(x) = e^{-x}$ in $OCPI_u$.

Theorem 2. *Let $\mu \in I_k, 1 \leq k \leq m$. As $L \rightarrow \infty$,*

$$E_{\mu}(T_C^*) \sim E_{\mu}(T'_k) \sim \frac{c'_k}{\delta_k(\mu - \frac{\delta_k}{2})}. \tag{4.5}$$

Furthermore, as $L \rightarrow \infty$, there exist the numbers, $\delta_1^* < \delta_2^* < \dots < \delta_m^*$, such that

$$OCPI_u(\delta_1^*, \dots, \delta_m^*) = \max_{\{\delta_k, 1 \leq k \leq m\}} \{CPI_u(\delta_1, \dots, \delta_m)\}, \tag{4.6}$$

and δ_1^* and δ_k^* are, respectively, the unique solutions to

$$\begin{aligned}
 I_1(x) &= \int_a^{\frac{x+\delta_2^*}{2}} \frac{(\mu-x)\mu^2}{x^2(\mu-\frac{x}{2})^2} d\mu = 0, \\
 I_k(x) &= \int_{\frac{\delta_{k-1}^*+x}{2}}^{\frac{x+\delta_{k+1}^*}{2}} \frac{(\mu-x)\mu^2}{x^2(\mu-\frac{x}{2})^2} d\mu = 0
 \end{aligned}
 \tag{4.7}$$

for $2 \leq k \leq m$, where $\delta_0^* = 0$, $a < \delta_1^* < 2a$ and $\delta_m^* < \delta_{m+1}^* = b$.

Remark 2. It follows from Theorem 1 and Section 3 of Lorden (1971) that

$$OCPI_u(\delta_1, \dots, \delta_k) < OCPI_u(\delta_1, \dots, \delta_{k+1})
 \tag{4.8}$$

for $k \geq 1$, and

$$\lim_{L \rightarrow \infty} \lim_{m \rightarrow \infty} OCPI_u(\delta_1, \dots, \delta_m) = 1
 \tag{4.9}$$

for $\delta_k = a + k(b - a)/(m + 1)$, $1 \leq k \leq m$.

The proof of Theorem 2 is in the appendix. By using (4.6) and (4.7) we can get an optimal design of the CUSUM multi-chart. The inequality (4.8) means that the $OCPI_u$ will increase if one more reference value that is greater than the existent reference values is added to T_C^* . From (4.9) it follows that the ARL of the CUSUM multi-chart, $ARL_\mu(T_C^*)$, can approximate the optimal ARL Curve, $ARL_r(\mu)$, if there are many reference values evenly distributed in the range $[a, b]$.

Let T_k and T_E denote, respectively, a one-sided CUSUM chart with the reference value δ_k ($1 \leq k \leq m$) and a one-sided EWMA chart with the reference value r ($0 < r \leq 1$).

Theorem 3. Let the numbers p_k satisfy $p_k > 0$ and $\sum_{k=1}^m p_k = 1$. If the CUSUM multi-chart, CUSUM and EWMA have a common $ARL_0 = L$, as $L \rightarrow \infty$,

$$\sum_{k=1}^m p_k E_\mu(T_k) > E_\mu(T_C^*),
 \tag{4.10}$$

and

$$E_\mu(T_E) > E_\mu(T_C^*),
 \tag{4.11}$$

for $\mu > \delta_1/2$.

Remark 3. Let T_{GL} be the one-sided GLR chart with $ARL_0 = L$. It follows from Section 3 of Lorden (1971), or Theorem 6 of Han and Tsung (2004), that $E_\mu(T_{GL}) \leq E_\mu(T_C^*)$. as $L \rightarrow \infty$.

The proof of Theorems 3 is in the appendix. From Theorem 3 we find that the CUSUM multi-chart has better performance than any single constituent

CUSUM chart in detecting an unknown mean shift. The CUSUM multi-chart is also better than the EWMA except in detecting the mean shift of a size less than $\delta_1/2$. Although the GLR is better than the CUSUM multi-chart, by Remark 3, when the ARL_0 goes to infinity, the simulation results given in Table 1 shows that the CUSUM multi-chart actually outperforms GLR in detecting small mean shifts when the ARL_0 is not large. As simulation results show, the good property of the multi-chart also holds when the ARL_0 is set at some typical value (e.g., 500) that is not large.

Table 1. ARLs and their standard errors (in parentheses) of the CUSUM charts with $ARL_0 = 500$.

SHIFTS (μ)	$\delta_1 = 0.1$ $c_1 = 1.979$	$\delta_2 = 0.5$ $c_2 = 4.29$	$\delta_3 = 1$ $c_3 = 5.075$	$\delta_4 = 1.5$ $c_4 = 5.337$	$\delta_5 = 2$ $c_5 = 5.355$
0	500(414)	500(491)	500(502)	500(490)	500(498)
0.1	239(169)	301(284)	369(366)	417(416)	439(433)
0.25	91.7(42.7)	94.2(77.2)	144(135)	202(198)	252(250)
0.5	44.2(14.3)	31.0(17.7)	38.9(31.8)	58.1(53.7)	81.9(78.8)
0.75	28.9(7.46)	17.5(7.55)	17.2(11.1)	22.0(17.9)	30.7(27.6)
1	21.5(4.74)	12.2(4.45)	10.5(5.56)	11.6(7.92)	14.6(11.9)
1.25	17.2(3.43)	9.34(2.96)	7.52(3.36)	7.53(4.37)	8.56(6.04)
1.5	14.3(2.59)	7.59(2.16)	5.83(2.29)	5.50(2.72)	5.80(3.59)
2	10.8(1.69)	5.55(1.32)	4.07(1.30)	3.56(1.41)	3.43(1.63)
3	7.27(0.93)	3.68(0.72)	2.60(0.66)	2.19(0.64)	1.95(0.71)
4	5.54(0.64)	2.84(0.51)	2.03(0.38)	1.64(0.51)	1.39(0.51)
$OCPI_k$	0.352	0.753	0.811	0.703	0.557
$OCPI_u$	0.245	0.651	0.743	0.662	0.538

4.3. Simulation results

Simulation results were based on a 10,000-repetition experiment. The common ARL_0 was chosen to be 500. We compare the simulation results for the ten mean shifts ($\mu_1 = 0.1, \mu_2 = 0.25, \dots, \mu_{10} = 4$) listed in the first column of the table with change point $\tau = 1$. The following tables illustrate the numerical results of ARLs of the two-sided CUSUM, EWMA, CUSUM multi-chart, EWMA multi-chart, GLR and the optimal CUSUM multi-charts. In order to compare the averages of $ARLs$ of the CUSUM and EWMA charts with those of the CUSUM and EWMA multi-charts, we at first list the simulation results of the CUSUM charts with the parameters, $\{\delta_1 = 0.1, \delta_2 = 0.5, \delta_3 = 1, \delta_4 = 1.5, \delta_5 = 2\}$ and EWMA charts with $\{r_1 = 0.1, r_2 = 0.3, r_3 = 0.5, r_4 = 0.7, r_5 = 0.9\}$ in Tables 1 and 2. In the first two rows, c denotes various values of the width of the control limits, and δ is the parameter of the CUSUM charts. The sizes of the mean shifts (μ) are listed in the first column of the tables. The values in parentheses are the standard deviations of the $ARLs$.

Table 2. ARLs and their standard errors (in parentheses) of the EWMA control chart with $ARL_0 = 500$.

SHIFTS (μ)	$r_1=0.1$ $c_1 = 2.818$	$r_2=0.3$ $c_2 = 3.026$	$r_3=0.5$ $c_3 = 3.073$	$r_4=0.7$ $c_4 = 3.085$	$r_5=0.9$ $c_5 = 3.089$
0	500(497)	500(495)	500(492)	500(504)	500(502)
0.1	320(316)	403(398)	438(431)	455(458)	470(473)
0.25	106(95.8)	187(181)	256(255)	308(311)	354(355)
0.5	31.2(22.2)	55.4(51.6)	88.7(87.4)	128(128)	176(178)
0.75	15.8(8.85)	22.5(18.9)	36.0(33.9)	55.5(54.6)	84.6(85.3)
1	10.3(4.78)	11.9(8.61)	17.4(15.3)	26.9(25.5)	42.7(42.1)
1.25	7.68(3.05)	7.65(4.73)	10.0(8.01)	14.7(13.4)	23.5(22.9)
1.5	6.10(2.15)	5.55(3.00)	6.53(4.64)	8.90(7.72)	13.7(13.1)
2	4.36(1.25)	3.55(1.48)	3.64(2.04)	4.30(3.12)	5.80(5.01)
3	2.87(0.67)	2.16(0.66)	1.92(0.78)	1.86(0.95)	1.98(1.28)
4	2.19(0.42)	1.61(0.52)	1.33(0.49)	1.23(0.45)	1.21(0.48)
$OCPI_k$	0.868	0.719	0.487	0.274	0.113
$OCPI_u$	0.787	0.682	0.478	0.285	0.128

Table 3. Comparison of the averages of ARLs of the CUSUM and EWMA charts with the ARLs of the multi-chart and GLR control charts with $ARL_0 = 500$ (with their standard errors shown in parentheses).

SHIFTS (μ)	Ave.CUSUM	CUSUM	Opt.CUSUM	Ave.EWMA	EWMA	$GLR(T_G)$
		Multi-chart	Multi-chart		Multi-chart	$c = 3.494$
0	500(479)	500(460)	500(477)	500(498)	500(499)	500(492)
0.1	353(334)	262(201)	272(229)	417(415)	381(374)	324(288)
0.25	157(141)	97.0(60.5)	96.3(60.1)	242(240)	146(135)	114(83.1)
0.5	50.8(39.3)	35.2(20.9)	35.8(20.4)	95.8(93.5)	40.1(31.0)	37.4(23.8)
0.75	23.2(14.3)	18.2(9.73)	18.8(10.0)	42.9(40.3)	18.2(11.3)	18.6(10.8)
1	14.1(6.92)	11.6(5.98)	11.86(6.16)	21.8(19.2)	11.2(6.08)	11.4(6.24)
1.25	10.0(4.03)	8.08(3.98)	8.22(4.11)	12.7(10.4)	7.81(3.95)	7.83(4.11)
1.5	7.81(2.67)	6.03(2.82)	6.11(2.95)	8.15(6.13)	5.85(2.91)	5.77(2.92)
2	5.48(1.47)	3.83(1.61)	3.80(1.75)	4.33(2.58)	3.68(1.77)	3.58(1.66)
3	3.54(0.73)	2.20(0.73)	2.01(0.84)	2.16(0.87)	1.92(0.89)	1.94(0.81)
4	2.69(0.51)	1.58(0.53)	1.34(0.51)	1.52(0.47)	1.28(0.49)	1.31(0.49)
$OCPI_u$	0.609	0.896		0.394	0.804	0.862
$OCPI_k$	0.531	0.865	0.8797	0.393	0.808	0.864

In Table 3, we compare the simulation results of the $ARL_{\mu}s$ for the GLR, CUSUM and EWMA multi-chart, and the averages of the $ARL_{\mu}s$ for five constituent CUSUM charts corresponding to the cases $\{\delta_1 = 0.1, \delta_2 = 0.5, \delta_3 = 1, \delta_4 = 1.5, \delta_5 = 2\}$. The Ave. CUSUM in the second column shows the average of ARLs for the constituent CUSUM charts from Table 1. In the third column,

to obtain the $ARL_0(T_C^*) = 500$ for the CUSUM multi-chart T_C^* , we take the control limits $c'_1 = 2.71$, $c'_2 = 5.22$, $c'_3 = 6.029$, $c'_4 = 6.282$ and $c'_5 = 6.301$ such that $ARL_0(T(\delta_1, c'_1)) = 1,297.4$, $ARL_0(T(\delta_2, c'_2)) = 1,298.5$, $ARL_0(T(\delta_3, c'_3)) = 1,298.6$, $ARL_0(T(\delta_4, c'_4)) = 1,297.2$ and $ARL_0(T(\delta_5, c'_5)) = 1,298.1$. The simulation results for the optimal CUSUM multi-chart are listed in the fourth column with the reference values δ_k^* chosen according to (4.6) and (4.7), that is, $\delta_1^* = 0.166$, $c'_1 = 3.64$; $\delta_2^* = 0.458$, $c'_2 = 5.24$; $\delta_3^* = 0.997$, $c'_3 = 6.177$; $\delta_4^* = 1.86$, $c'_4 = 6.458$; $\delta_5^* = 3.126$, $c'_5 = 6.202$, where the control limits c'_k are taken for $ARL_0(T_C^*) = 500$. More discussion on the optimal CUSUM multi-chart is in Section 5. Also, in the fifth and the sixth columns, we have Ave. EWMA, which gives the average of ARLs for the constituent EWMA charts from Table 2, and the EWMA multi-chart T_E^* . Moreover, we list the simulation results of the GLR (T_{GL}) in the last column with the control limit $c = 3.494$, which leads to the same ARL_0 value.

The bottom two rows of each table list the $OCPI_k$ and $OCPI_u$ values for different charts, where we take $f(x) = e^{-x}$ in the $OCPI$. These represent the OCPI values under known and unknown shifts, respectively. $OCPI_k$ is calculated based on the five anticipated shift sizes of 0.1, 0.5, 1, 1.5 and 2, assuming that the actual mean shifts are consistent with the anticipated mean shifts. Here the reference optimal ARL curve, $ARL_r(\mu)$, is taken as the ARL 's of the CUSUM chart, that is,

$$\begin{aligned} ARL_r(0) &= 500, ARL_r(0.1) = 239, ARL_r(0.25) = 82.95, ARL_r(0.5) = 31.02, \\ ARL_r(0.75) &= 16.54, ARL_r(1) = 10.53, ARL_r(1.25) = 7.386, ARL_r(1.5) = 5.496, \\ ARL_r(2) &= 3.432, ARL_r(3) = 1.793, ARL_r(4) = 1.204. \end{aligned}$$

$OCPI_u$ should be calculated based on all possible mean shifts in a range. Here, the simplified calculation is based on all the mean shifts listed in the first column to represent the performance for a range of unknown mean shifts.

Our findings based on the comparison of the numerical results are summarized as follows. The results in Table 1 show that each of the five constituent CUSUM charts is good for its designed optimal shift as expected, while the $OCPI_k$ and $OCPI_u$ values that represent the overall performance over a range vary according to the designed parameters. In both the situations with known and unknown mean shifts in an anticipated range, the optimal CUSUM multi-chart is consistently better than any of the single constituent CUSUM charts in terms of the $OCPI_k$ and $OCPI_u$ values, as shown in Table 3. Table 3 also indicates that the performance of CUSUM multi-charts is consistently better than the average performance of the constituent CUSUM charts in the sense that the average ARLs of the constituent charts is always larger than the ARLs of the

multi-charts. Compared with GLR charts, the CUSUM multi-chart has a higher *OCPI* value when the mean shifts are known, and is only slightly better when the shifts are unknown. Moreover, Tables 2 and 3 show that the EWMA multi-chart is not as good as the CUSUM multi-chart and the GLR chart, and one EWMA chart with $r=0.1$ seems to perform particularly well for a range of known shifts. However, the performance of the EWMA multi-chart is consistently better than the average performance of the constituent EWMA charts as the average ARLs of the EWMA charts are always larger than the ARLs of the EWMA multi-charts.

Finally, an interesting result in Table 3 is that the standard deviations of the ARLs for the CUSUM multi-chart are the smallest among the six charts, except when detecting the mean shift $\mu = 4$.

5. Design of a Multi-Chart

Although we have proved the optimal property of the CUSUM multi-chart, the superior performance of the multi-chart still requires an effective design. For the situation with known anticipated mean shifts, we can design the multi-chart by combining those constituent charts specifically designed for each anticipated mean shift size. With an unknown mean shift in a range, we can also determine how many constituent charts to combine and where to locate them according to a desirable OCPI. This section will examine this problem via theoretical calculation and Monte Carlo simulation, and provide a general guideline for the design of a CUSUM multi-chart and an EWMA multi-chart.

5.1. Design of a CUSUM Multi-Chart

We first focus on the design of the CUSUM multi-chart. Here, four design schemes are proposed. Denote the anticipated range as $[a,b]$, and suppose n constituent CUSUM charts are to be used. Let p_i be the proportion of the position of each constituent chart within the range and δ_i be the placement location. The design schemes are described as the following.

1. An optimal placement scheme. Let $a = 0.1, b = 4$. By using (4.7) we can obtain the theoretical optimal reference values δ_k^* for $n = 2, 3, 4$ and 5, such that $OCPI_u$ attains its maximum value, $OCPI_u^*$. Thus for

$$\begin{aligned} n=2, \delta_1^* &= 0.1948, \delta_2^* = 1.6207, OCPI_u^* = 0.7152; \\ n=3, \delta_1^* &= 0.184, \delta_2^* = 0.852, \delta_3^* = 2.474, OCPI_u^* = 0.8927; \\ n=4, \delta_1^* &= 0.172, \delta_2^* = 0.585, \delta_3^* = 1.433, \delta_4^* = 2.886, OCPI_u^* = 0.9438; \\ n=5, \delta_1^* &= 0.166, \delta_2^* = 0.458, \delta_3^* = 0.997, \delta_4^* = 1.86, \delta_5^* = 3.126, \\ &OCPI_u^* = 0.96518. \end{aligned}$$

The theoretical value $OCPI_u^* = 0.96518$ of the optimal CUSUM multi-chart for $n = 5$ is high. The simulation result in Table 3 confirms that the optimal CUSUM multi-chart with the five CUSUM charts has the best performance among the six control charts in terms of $OCPI_k$, even though the ARL_0 is not large.

2. Even placement scheme. Take

$$p_i = \frac{i}{n+1}, \quad \delta_i = a + (b-a) \cdot p_i. \tag{5.1}$$

As shown in Figure 2 (a), the constituent charts are evenly distributed in the anticipated range.

3. Side-concentrated placement scheme. Take

$$p_i = \frac{\tau^i - 1}{\tau^{(n+1)} - 1}, \quad \delta_i = a + (b-a) \cdot p_i. \tag{5.2}$$

As shown in Figure 2 (b) and (c), the emphasis of the multi-chart is on the extremes. If $\tau > 1$, the charts concentrate on the lower end, while if $\tau < 1$, the charts will concentrate on the higher end.

4. Center-concentrated placement scheme. Take

$$p_i = \begin{cases} \frac{\tau^i - 1}{2[\tau^{\frac{n}{2}} - 1] + \tau^{\frac{n}{2}}(\tau - 1)} & \text{if } n \text{ is even and } i \leq \frac{n}{2} \\ \frac{\tau^{n-i+1} - 1}{2[\tau^{\frac{n}{2}} - 1] + \tau^{\frac{n}{2}}(\tau - 1)} & \text{if } n \text{ is even and } i > \frac{n}{2} \\ \frac{\tau^i - 1}{2[\tau^{\frac{n+1}{2}} - 1]} & \text{if } n \text{ is odd and } i \leq \frac{n}{2} \\ \frac{\tau^{n-i+1} - 1}{2[\tau^{\frac{n+1}{2}} - 1]} & \text{if } n \text{ is odd and } i > \frac{n}{2} \end{cases} \tag{5.3}$$

$$\delta_i = a + (b-a) \cdot p_i.$$

Figure 2 (d) and (e) show a scheme that emphasizes the center or both ends. If $\tau > 1$, the charts will concentrate on the ends; if $\tau < 1$, the charts concentrate on the center of the anticipated range.

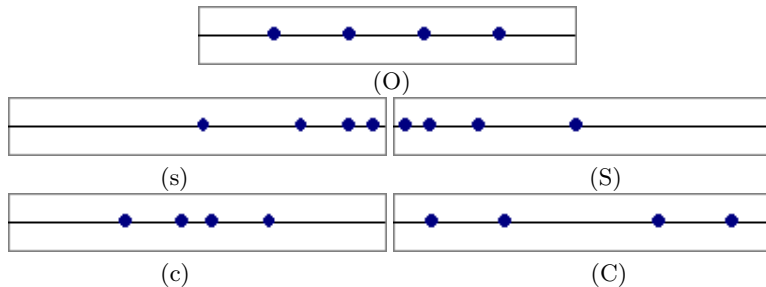


Figure 2. Placement of four CUSUM Charts. (O) Even placement. (s) Side-concentrated, $\tau = 0.5$. (S) Side-concentrated, $\tau = 2.0$. (c) Center-concentrated, $\tau = 0.5$. (C) Center-concentrated, $\tau = 2.0$.

Here the simulation is conducted based on the three different design schemes. The anticipated shift range is selected as (0,3), and the OCPI is used as a criterion for performance evaluation. The results are shown in Figure 3.

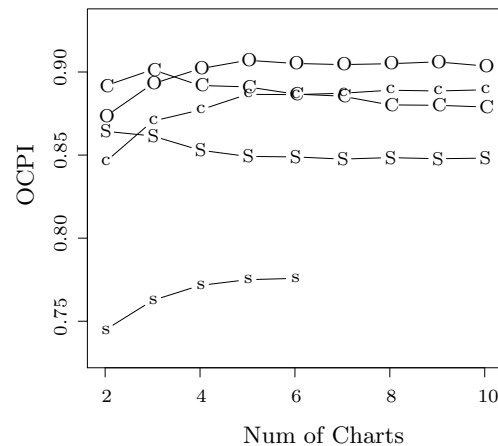


Figure 3. OCPI curve of multi-CUSUM. (s) Side-concentrated, $\tau = 0.5$. (S) Side-concentrated, $\tau = 2.0$. (c) Center-concentrated, $\tau = 0.5$. (C) Center-concentrated, $\tau = 2.0$. (O) Even placement. Note: An unfinished curve exists because its placement is too close to zero.

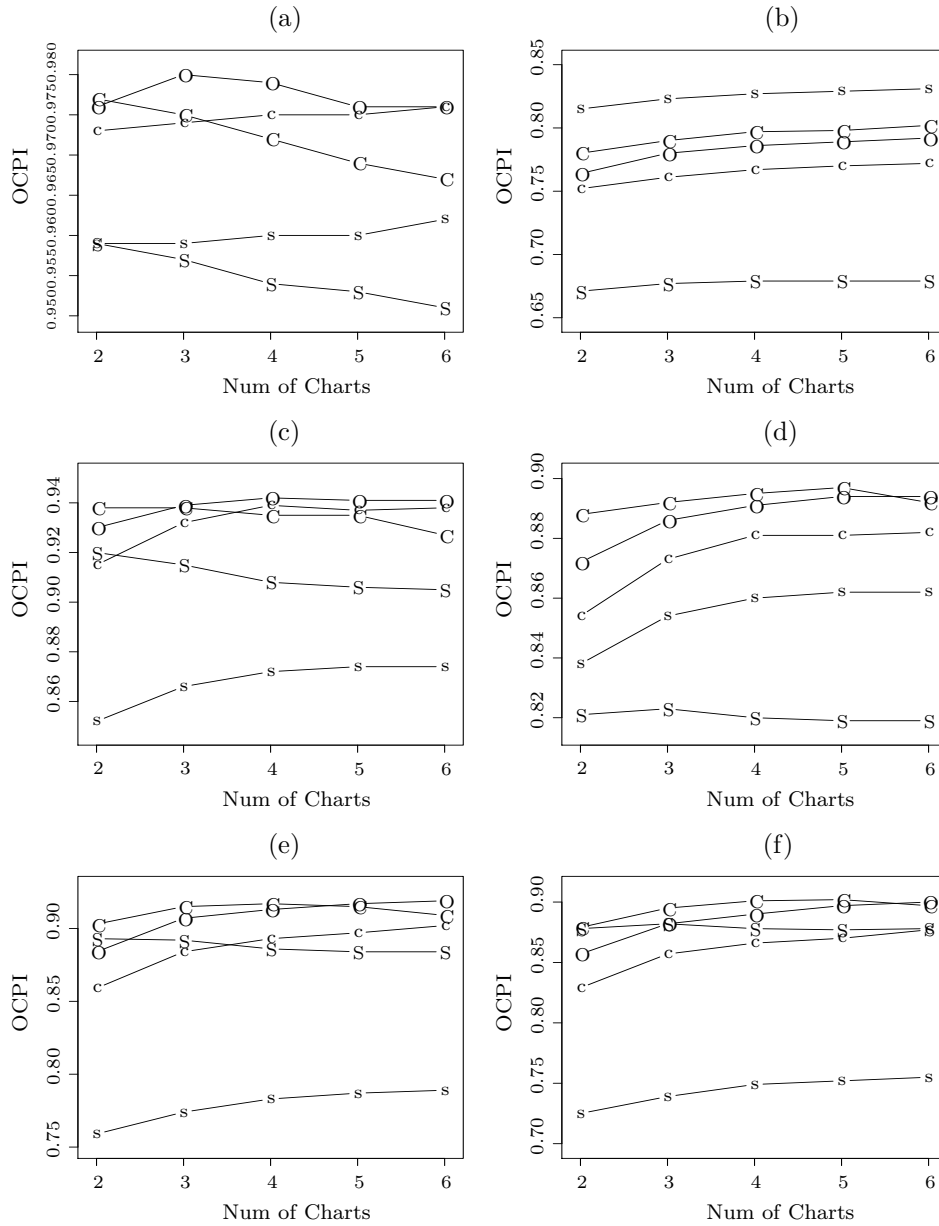
One can see that when the number of constituent CUSUM charts is no more than three, the center-concentrated scheme with $\tau = 2.0$ gives the highest OCPI value. When the number of charts is larger than three, the even placement scheme shows the best performance.

Another notable phenomenon is that the OCPI does not always increase with the number of charts. For C2.0 and S2.0 placement schemes, the OCPI actually decreases when using more than four charts. For the even placement scheme, the OCPI value is stabilized with minor fluctuation when more than five charts are used. Also, the ARL curve of s0.5 is always far below the others, which turns out to be the worst scheme.

Thus, for the situation with an anticipated shift range (0, 3), we conclude that placing the constituent charts evenly along the anticipated range should give a reasonably good result with more than three charts. If no more than three constituent charts are used, putting some on the lower side and some on the higher side should generate good performance. Also, the OCPI curve provides an indication for the chart number determination. In this case, we suggest no more than five constituent charts, as the OCPI curve becomes flat after that.

With different anticipated mean shift ranges, we conduct more extensive simulations by choosing several usual anticipated mean shift ranges for the design,

with the actual mean shifts either within or outside the design range, as in Figure 4. For example, if the design range is $[0.2, 1]$ and expected shifts fall into the same range, the even placement scheme with three CUSUM charts should be used since it indicates the highest OCPI value and the curve goes flat or downwards after that.



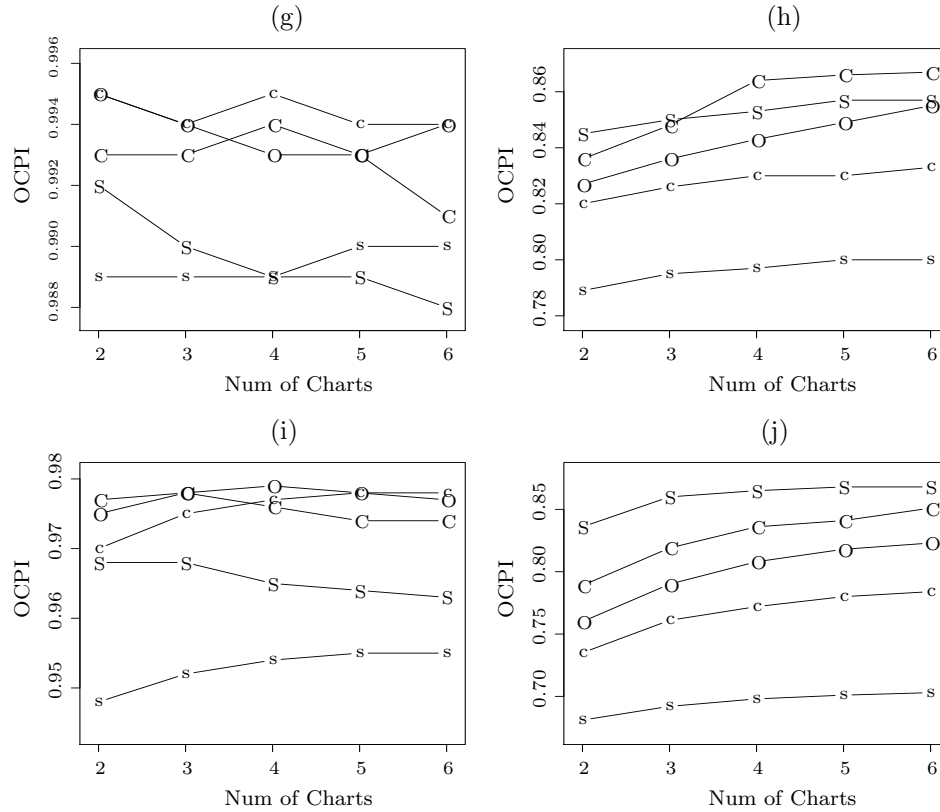


Figure 4. Simulation results of multi-CUSUM. (a) Design: 0.2-1, Shift: 0.2-1. (b) Design: 0.2-1, Shift: 0-3. (c) Design: 0.2-2, Shift: 0.2-2. (d) Design: 0.2-2, Shift: 0-3. (e) Design: 0.2-3, Shift: 0.2-3. (f) Design: 0.2-3, Shift: 0-3. (g) Design: 1-2, Shift: 1-2 (h) Design: 1-2, Shift: 1-3. (i) Design: 1-3, Shift: 1-3. (j) Design: 1-3, Shift: 1-3. Legend: (s) side-concentrated, $\tau = 0.5$; (S) side-concentrated, $\tau = 2.0$; (c) center-concentrated, $\tau = 0.5$; (C) center-concentrated, $\tau = 2.0$; (O) even placement.

5.2. Design of an EWMA Multi-Chart

Here, we investigate the design of EWMA multi-chart. To design an EWMA multi-chart that combines several constituent EWMA charts, we need to look into the smoothing coefficient of EWMA, r . We call the smoothing coefficient the “location” of an EWMA chart. The same placement schemes can then be applied as in the CUSUM multi-chart, except that now the range of placement is (0,1) since r cannot exceed 1.

Figure 5 shows the OCPIs of different design schemes for EWMA multi-charts. One can see that the S2.0 scheme shows the best ARL performance when the number of charts is less than seven, the C2.0 scheme catches up when

the number of charts is more than seven, while the s0.5 scheme gives the worst performance.

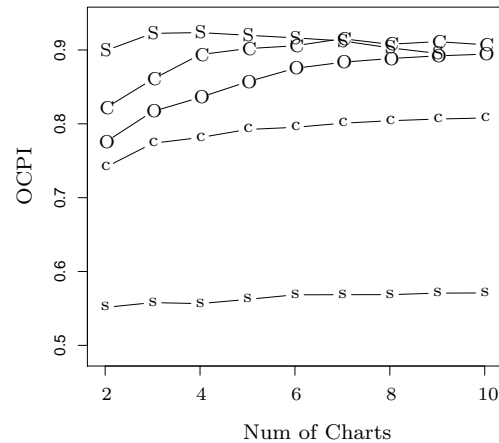


Figure 5. OCPI curve of multi-EWMA. Legend: (s) side-concentrated, $\tau = 0.5$; (S) side-concentrated, $\tau = 2.0$; (c) center-concentrated, $\tau = 0.5$; (C) center-concentrated, $\tau = 2.0$; (O) even placement. Note: An unfinished curve exists because its placement is too close to zero.

We conclude that in this case we should choose the smoothing parameter r close to 0 if fewer than seven charts are to be used. If more than seven charts are used, some r 's should be close to 0, and some close to 1. The simulation results also show that the OCPI curve flattens and goes downwards after three charts, which indicates that no more than three charts is useful.

5.3. Discussion on Design Guidelines

From the results of Monte Carlo experiments for the CUSUM multi-charts and the EWMA multi-charts, we can see that the performance does not always increase by adding more charts if the reference values of the added CUSUM charts are less than the existent reference values. We may recommend the number of constituent charts by finding the initial flat or downward point on the OCPI curve. The allocation of the constituent charts then follows the corresponding placement scheme that generates the best OCPI value.

The ARL calculation of a multi-chart can also be done by numerical methods. The single CUSUM ARL numerical method by Brook and Evans (1972) and the single EWMA ARL numerical method by Lucas and Saccucci (1990) can be easily extended to a multi-chart scenario. For each single chart, we discretize the range between control limits. A Markov chain can be formed by taking the

state as a multidimensional vector $(E_1, \dots, E_n)'$, where E_i is the state of the i th chart, n is the total number of charts in use. If each chart is discretized into t intervals, the transition matrix of the Markov chain is a $(t+1)^n \times (t+1)^n$ matrix. Brook and Evans (1972) recommended $t = 5$ for a reasonably good result. For a multi-chart, the dimension of this matrix grows exponentially. If $n = 4$ charts with $t = 5$, the dimension of the transition matrix will be $1,296 \times 1,296$, which will be very difficult to manipulate. Thus, in this paper, all results are obtained by Monte Carlo experiments only.

6. Conclusion

We have mainly discussed the CUSUM and EWMA multi-chart schemes to handle the situation with an anticipated range of known or unknown process changes by combining the strengths of multiple charts. We show that the multi-chart has the merits of quick detection of a range of mean shifts, easy and flexible design for various situations, and great reduction in computational complexity. In particular, we have proved the asymptotic optimality of the CUSUM multi-chart in detecting more than one possible mean shift in a range. Also, the numerical simulation results show that the CUSUM multi-chart is more efficient and robust on the whole than the CUSUM, EWMA and EWMA multi-chart in terms of OCPI, and can perform as well as the GLR chart in detecting various mean shifts when the in-control ARL is not large.

The charting performance of a multi-chart depends on the design of the multi-chart parameters including the number of constituent charts and the allocation of their reference values. We have provided an optimal design of the CUSUM multi-chart and some practical guideline for both CUSUM and EWMA multi-charts based on the OCPI curve with different placement schemes. Note that the multi-chart has great flexibility in taking various forms of its constituent charts to further improve its performance. The design and analysis of the multi-chart with mixed forms of charts warrant future research.

As can be seen that the results considered in the paper are from the initial state, $\mu_0 = 0$. It would be interesting to investigate whether the results are similar if the shifts are generated from a steady state, e.g., shifts are generated after the CUSUM is allowed to run through several in-control values. The intuitive idea is that the results should be similar if all the mean shifts μ and the reference values δ_k are greater than $\mu_0 = \max\{\text{several in-control values}\}$ when the ARL_0 is large. However, it seems difficult to prove the intuitive idea since it is not easy to choose a proper " ARL_0 " for the several in-control values. Similarly, it should be anew considered whether the optimality properties of Moustakeides (1986) in Lorden's sense (1971) still holds when the CUSUM chart is allowed to run through several in-control values.

Moreover, in recent years, adaptive CUSUM (Sparks (2000)) and adaptive EWMA (Capizzi and Masarotto (2003)) have been proposed in the literature to achieve the same aim as in the paper. It is worthwhile to compare these charts on which is more efficient in detecting a group of unknown mean shifts.

Acknowledgements

We thank the Editor and two referees for their valuable comments and suggestions that have improved this work. This work was supported by RGC Competitive Earmarked Research Grants HKUST6232/04E and HKUST6204/05E.

Appendix

Proof of Theorem 1. Since $T_C^* \leq T'_i$ for all $1 \leq i \leq n$, it follows that

$$\frac{2 \log L'}{\mu_i^2} + M(\mu_i) + o(1) = E_{\mu_i}(T'_i) \geq E_{\mu_i}(T_C^*) \geq E_{\mu_i}(T_i) = \frac{2 \log L}{\mu_i^2} + M(\mu_i) + o(1)$$

for all $1 \leq i \leq n$ as $L \rightarrow \infty$, where $o(1) = O(L^{-1} \ln(\mu^2 L/2))$. Thus, Theorem 1 is true if $\log L' - \log L \leq O((\ln L)^3/L) = O(c_1^3 e^{-c_1})$ as $L \rightarrow \infty$, or as $\min_{1 \leq i \leq n} \{c_i\} \rightarrow +\infty$. It is known that (see Srivastava and Wu (1997))

$$L' = E_0(T'_i) = \frac{e^{(c'_i + 2\delta_i\rho)} - 1 - (c'_i + 2\delta_i\rho)}{\frac{\delta_i^2}{2}} + O(\delta_i) \tag{A.1}$$

for large c'_i , $1 \leq i \leq n$, where $\rho \approx 0.583$. Denote by φ and Φ the standard normal density and distribution functions, respectively. Let $U_m(k) = [X_m + \dots + X_{m-k+1}]/k^{1/2}$, $1 \leq k \leq m$. Then the stopping time T'_i can be written

$$T'_i = \min \left\{ n : \max_{1 \leq k \leq n} \left[U_n(k) > \frac{c'_i}{\delta_i \sqrt{k}} + \frac{\delta_i}{2} \sqrt{k} \right] \right\}. \tag{A.2}$$

From (A.1) and (A.2), it follows that

$$\frac{c'_1}{\delta_1} > \frac{c'_2}{\delta_2} > \dots > \frac{c'_m}{\delta_m}, \tag{A.3}$$

$$c'_i - c'_j = (1 + o(1))(c_i - c_j) = (1 + o(1)) \left[2 \ln \left(\frac{\delta_i}{\delta_j} \right) + (\delta_i - \delta_j)\rho \right], \tag{A.4}$$

for large $\min_{1 \leq k \leq n} \{c_k\}$. We first show that

$$0 \leq E_0(T'_1) - E_0(T_C^*) \leq A(c'_1)^3 + B \tag{A.5}$$

for large c'_1 , where A and B are two constants not depending on $c'_i, 1 \leq i \leq n$. The left inequality of (A.5) is obvious since $T_C^* \leq T'_1$. Note that

$$\begin{aligned}
 E_0(T'_1) &= \sum_{n=1}^{+\infty} P_0(T'_1 \geq n) \\
 &= \sum_{n=1}^{+\infty} P_0\left(U_n(k) < c'_1/(\delta_1\sqrt{k}) + (\delta_1/2)\sqrt{k}, 1 \leq k \leq l, 1 \leq l \leq n\right), \\
 E_0(T_C^*) &= \sum_{n=1}^{+\infty} P_0(T_C^* \geq n) \\
 &= \sum_{n=1}^{+\infty} P_0\left(U_n(k) < \min_{1 \leq i \leq m} \{c'_i/(\delta_i\sqrt{k}) + (\delta_i/2)\sqrt{k}\}, 1 \leq k \leq l, 1 \leq l \leq n\right).
 \end{aligned}$$

Since $c'_i/(\delta_i\sqrt{k}) + (\delta_i/2)\sqrt{k}$ attains its minimum value, $\sqrt{2c'_i}$, at $k = 2c'_i/(\delta_i)^2$, it follows from (A.3) that $|P_0(T'_1 \geq n) - P_0(T_C^* \geq n)| \leq n^2[1 - \Phi(\sqrt{2c'_1})]$ for $1 \leq n \leq 2c'_1/(\delta_1)^2$, and $|P_0(T'_1 \geq n) - P_0(T_C^* \geq n)| \leq (c'_1)^2/(\delta_1)^4[1 - \Phi(\sqrt{2c'_1})]$ for $2c'_1/(\delta_1)^2 < n \leq n'$, where $n' = c'_1 \exp\{c'_1\}$. Note that $1 - \Phi(\sqrt{2c'_1}) = O((\sqrt{2c'_1} \exp\{c'_1\})^{-1})$ for large c'_1 . Thus,

$$\sum_{n=1}^{n'} \left| P_0(T'_1 \geq n) - P_0(T_C^* \geq n) \right| \leq A(c'_1)^3 \tag{A.6}$$

for large c'_1 . On the other hand (see Siegmund (1985, p.25)), the stopping time $T'_1 = N_1 + \dots + N_K = K((\sum_{i=1}^K N_i)/K)$, where $\{N_i\}$ is dependent and identically distributed with mean $E(N_1) = b \leq O(c'_1)$ and K is geometrically distributed with mean $E(K) = O(b^{-1} \exp\{c'_1\})$ for large c'_1 . Hence, we have

$$\begin{aligned}
 \sum_{n=n'+1}^{+\infty} P_0(T'_1 \geq n) &\leq O\left(\sum_{n=n'+1}^{+\infty} P_0\left(K \geq \frac{n}{c'_1}\right)\right) \\
 &= O\left(\exp\{c'_1\}\left(1 - \frac{bc'_1}{n'}\right)^{\frac{n'}{b}}\right) \leq B
 \end{aligned} \tag{A.7}$$

for large c'_1 . By using (A.6) and (A.7), we see that (A.5) holds. Since $E_0(T_1) = L = E_0(T_C^*)$, it follows from (A.5) that

$$\begin{aligned}
 \left| \frac{E_0(T'_1) - E_0(T_C^*)}{E_0(T_1)} \right| &= |e^{(c'_1 - c_1)} - 1| \\
 &\leq (\delta_1)^2 [A(c'_1)^3 + B] e^{-(c_1 + 2\delta_1\rho)} \rightarrow 0
 \end{aligned}$$

as $L \rightarrow \infty$, otherwise we have a contradiction. This means that $c'_1 - c_1 \rightarrow 0$ as $L \rightarrow +\infty$. Note that $e^{(c'_1 - c_1)} - 1 = c'_1 - c_1 + o(c'_1 - c_1)$ and $\log L' - \log L =$

$c'_1 - c_1 + O(c'_1 e^{-c_1}) + O(c_1 e^{-c_1})$. Thus

$$\begin{aligned} \log L' - \log L &\leq (\delta_1)^2 [A(c'_1 - c_1 + c_1)^3 + B] e^{-(c_1 + 2\delta_1 \rho)} \\ &= O(c_1^3 e^{-c_1}) = O\left(\frac{(\ln L)^3}{L}\right), \end{aligned}$$

and this completes the proof.

Proof of Theorem 2. Let $j \neq k$ and $\mu \in I_k$. Note that $\mu > \delta_k/2$ since $\delta_{k-1} + \delta_k)/2 < \mu \leq (\delta_k + \delta_{k+1})/2$ and $\delta_{k-1} \geq 0$. Thus, the number μ must satisfies one of the following: (i) $\delta_k/2 < \mu \leq \delta_j/2$; (ii) $\delta_k/2 < \delta_j/2 < \mu$; (iii) $\mu > \delta_k/2 > \delta_j/2$. It follows from (4.1) and (A.1) that $c_j = c_k + C_{jk} + o(1)$ for large L , where $C_{jk} = \log[\delta_j^2/\delta_k^2]$. By the Strong Law of Large Numbers we have

$$\max_{1 \leq i \leq n} \frac{1}{n} \sum_{l=n-i+1}^n \delta_k [X_l(\omega) - \frac{\delta_k}{2}] \rightarrow \max\{0, \delta_k(\mu - \frac{\delta_k}{2})\}, \quad a.s. - P_\mu \quad (\text{A.8})$$

for $1 \leq k \leq m$ as $n \rightarrow \infty$. Note that

$$T(\delta_l) = T(\delta_l, \omega) \rightarrow \infty \quad a.s. - P_\mu \quad (\text{A.9})$$

for all $1 \leq k \leq m$ as $L \rightarrow \infty$. Thus, without loss of generality, we assume that (A.8) and (A.9) hold for all $\omega \in \Omega$, where $P_\mu(\Omega) = 1$. Assume that there is a $\omega \in \Omega$ such that $T_k = T(\delta_k, \omega) \geq T_j = T(\delta_j, \omega)$. This means that

$$\begin{aligned} \max_{1 \leq i \leq T_j} \frac{1}{T_j} \sum_{l=T_j-i+1}^{T_j} \delta_j [X_l - \frac{\delta_j}{2}] &> \frac{c_j}{T_j} = \frac{c_k + C_{jk} + o(1)}{T_j} \\ &\geq \frac{C_{jk} + o(1)}{T_j} + \frac{T_k - 1}{T_j} \max_{1 \leq i \leq T_k-1} \frac{1}{T_k - 1} \sum_{l=T_k-1-i+1}^{T_k-1} \delta_k [X_l - \frac{\delta_k}{2}], \quad (\text{A.10}) \end{aligned}$$

since $\max_{1 \leq i \leq T_k-1} \sum_{l=T_k-1-i+1}^{T_k-1} \delta_k [X_l - \delta_k/2] \leq c_k$ and $\max_{1 \leq i \leq T_j} \sum_{l=T_j-i+1}^{T_j} \delta_j [X_l - \delta_j/2] > c_j$ Thus, it follows from (A.8), (A.9) and (A.10) that

$$\max\{0, \delta_j(\mu - \frac{\delta_j}{2})\} \geq \max\{0, \delta_k(\mu - \frac{\delta_k}{2})\} \quad (\text{A.11})$$

as $L \rightarrow \infty$. This contradicts, $\delta_j/2 \geq \mu > \delta_k/2$, case (i). This means that the assumption $T_k = T(\delta_k, \omega) \geq T_j = T(\delta_j, \omega)$ is not true. Similarly, for the cases (ii) and (iii), it follows from (A.11) that $\delta_j(\mu - \delta_j/2) \geq \delta_k(\mu - \delta_k/2)$, that is, $\mu \geq (\delta_j + \delta_k)/2$, case (ii), and $\mu \leq (\delta_j + \delta_k)/2$, case (iii). Note that $\mu \in I_k$, It follows that

$$\mu > \frac{\delta_k + \delta_{k-1}}{2} = \frac{\delta_k + \delta_j}{2} + \frac{\delta_{k-1} - \delta_j}{2} \geq \frac{\delta_k + \delta_j}{2}$$

for case (iii), since $\delta_{k-1} \geq \delta_j$. This contradicts $\mu \leq (\delta_j + \delta_k)/2$. Similarly, by $\mu \in I_k$ we have $\mu \leq (\delta_k + \delta_j)/2 + (\delta_{k+1} - \delta_j)/2 \leq (\delta_k + \delta_j)/2$ for case (ii) since $\delta_{k+1} \leq \delta_j$. But $\mu \geq (\delta_k + \delta_j)/2$ for case (ii), so $\delta_{k+1} \delta_j$ and $\mu = (\delta_k + \delta_{k+1})/2$. In this case, $\delta_{k+1}(\mu - \delta_{k+1}/2) = \delta_k(\mu - \delta_k/2)$. Thus, we have $T_{k+1} \sim c_{k+1}/[\delta_{k+1}(\mu - \delta_{k+1}/2)]$ and $T_k \sim c_k/[\delta_k(\mu - \delta_k/2)]$ as $L \rightarrow \infty$. In fact, $\max_{1 \leq l \leq T_k} (T_k)^{-1} \sum_{i=T_k-l+1}^{T_k} \delta_k [X_i - \delta_k/2] > c_k/T_k$ and $\max_{1 \leq l \leq T_{k-1}} (T_k - 1)^{-1} \sum_{i=T_k-l}^{T_k-1} \delta_k [X_i - \delta_k/2] \leq c_k/T_k$. This implies that $T_k \sim c_k/[\delta_k(\mu - \delta_k/2)]$ for all $\omega \in \Omega$ as $L \rightarrow \infty$. Similar result can be obtained for T_{k+1} . So $T_j = T_{k+1} > T_k$ as $L \rightarrow \infty$ since $c_{k+1} > c_k$. This contradicts the assumption $T_j = T_{k+1} \leq T_k$ as $L \rightarrow \infty$. Thus we have $T(\delta_j) > T(\delta_k)$, a.s. P_μ , for $j \neq k$ and $\mu \in I_k$ as $L \rightarrow \infty$. Similarly, $T'(\delta_j) > T'(\delta_k)$, a.s. P_μ , for $j \neq k$ and $\mu \in I_k$ as $L \rightarrow \infty$. Hence $T_C^* = T_k'$, a.s. P_μ , for $\mu \in I_k$ as $L \rightarrow \infty$. Since the family $\{T_k'/c_k', c_k' > 0\}$ is uniformly integrable with respect to P_μ , so is $\{T_C^*/c_k', c_k' > 0\}$. Hence, as $L \rightarrow \infty$, $E_\mu(T_C^*) \sim E_\mu(T_k') \sim c_k'/[\delta_k(\mu - \delta_k/2)]$ for $\mu \in I_k$. Thus, (4.5) of Theorem 2 is established.

Since $c'_k - c_k \rightarrow 0$, $APL_r(\mu) \sim 2c_k/\mu^2$ and $APL_\mu(T_C^*) = E_\mu(T_C^*) \sim E_\mu(T_k') \sim c_k'/[\delta_k(\mu - \delta_k/2)]$ as $L \rightarrow \infty$ for $\mu \in I_k, 1 \leq k \leq m$,

$$\begin{aligned} CPI_u(\delta_1, \dots, \delta_k) &= \exp \left\{ \frac{-1}{b-a} \int_a^b \frac{APL_\mu(T_C^*) - ARL_r(\mu)}{ARL_r(\mu)} d\mu \right\} \\ &= (1 + o(1)) \exp \left\{ \frac{-1}{b-a} F(\delta_1, \dots, \delta_k) + 1 \right\} \end{aligned}$$

as $L \rightarrow \infty$, where

$$\begin{aligned} F(\delta_1, \dots, \delta_k) &= \frac{1}{2} \left[\int_a^{\frac{\delta_1 + \delta_2}{2}} \frac{\mu^2}{\delta_1(\mu - \frac{\delta_1}{2})} d\mu + \sum_{i=2}^{k-1} \int_{\frac{\delta_{i-1} + \delta_i}{2}}^{\frac{\delta_i + \delta_{i+1}}{2}} \frac{\mu^2}{\delta_i(\mu - \frac{\delta_i}{2})} d\mu \right. \\ &\quad \left. + \int_{\frac{\delta_{k-1} + \delta_k}{2}}^b \frac{\mu^2}{\delta_k(\mu - \frac{\delta_k}{2})} d\mu \right]. \end{aligned}$$

It follows that

$$\frac{\partial CPI_u(\delta_1, \dots, \delta_k, \dots, \delta_m)}{\partial \delta_k} = - \exp \left\{ \frac{-1}{b-a} F + 1 \right\} \frac{\partial F(\delta_1, \dots, \delta_k, \dots, \delta_m)}{\partial \delta_k}$$

and

$$\frac{\partial F}{\partial \delta_1} - \int_a^{\frac{\delta_1 + \delta_2}{2}} \frac{(\mu - \delta_1)\mu^2}{2\delta_1^2(\mu - \frac{\delta_1}{2})^2} d\mu, \quad \frac{\partial F}{\partial \delta_k} - \int_{\frac{\delta_{k-1} + \delta_k}{2}}^{\frac{\delta_k + \delta_{k+1}}{2}} \frac{(\mu - \delta_k)\mu^2}{2\delta_k^2(\mu - \frac{\delta_k}{2})^2} d\mu.$$

for $2 \leq k \leq m$. It can be checked that $\partial F/\partial \delta_k < 0$ as δ_k approximates δ_{k-1} and $\partial F/\partial \delta_k > 0$ as δ_k approximate δ_{k+1} ; similarly, it is true for $\partial F/\partial \delta_1$, and

$$\frac{\partial^2 F}{\partial^2 \delta_k} \frac{(\delta_{k+1} - \delta_{k-1})[\delta_k^3 + \delta_{k-1}\delta_{k+1}(\delta_{k-1} + \delta_k + \delta_{k+1})]}{8\delta_{k-1}\delta_{k+1}\delta_k^3} > 0$$

for $2 \leq k \leq m$. Hence, there exist a unique series of numbers, $\delta_k^*, 1 \leq k \leq m$, such that $a < \delta_1^* < 2a, \delta_k^* < \delta_{k+1}^* < b$ for $1 \leq k \leq m - 1$, and $F(\delta_1, \dots, \delta_k, \dots, \delta_m)$ attains its minimum value at $\delta_1^*, \dots, \delta_k^*, \dots, \delta_m^*$, that is, CPI_u attains its maximum value at $\delta_1^*, \dots, \delta_k^*, \dots, \delta_m^*$. This completes the proof of Theorem 2.

Proof of Theorem 3. Let $T(\delta, c)$ denote the CUSUM chart with reference value δ and control limit c . It is known that (see Srivastava and Wu (1997)), as $L \rightarrow \infty$,

$$E_\mu(T(\delta, c)) = (1 + o(1)) \frac{e^{(\delta-2\mu)(c+2\delta\rho)\delta^{-1}} - 1 - (\delta - 2\mu)(c + 2\delta\rho)\delta^{-1}}{2(\mu - \frac{\delta}{2})^2}$$

for $\delta > 2\mu, E_\mu(T(\delta, c)) = (1 + o(1))(c^2/\delta^2)$ as $\delta \rightarrow 2\mu$, and $E_\mu(T(\delta, c)) = (1 + o(1))[2c/\delta(2\mu - \delta)]$ for $\delta < 2\mu$. Hence, by $\log L' - \log L \rightarrow 0$, or $c' - c \rightarrow 0$ as $L \rightarrow \infty$, we have

$$E_\mu(T'_i) = (1 + o(1))E_\mu(T_i) \tag{A.12}$$

for $1 \leq i \leq m$. (i). If $\delta_i > 2\mu, 1 \leq i \leq m$, then $(\delta_i - 2\mu)/\delta_i > (\delta_j - 2\mu)/\delta_j$ for $i > j$, and therefore, by (A.12),

$$\begin{aligned} E_\mu(T_i) &= (1 + o(1)) \left[\frac{e^{(\delta_i-2\mu)(c_i+2\delta_i\rho)/\delta_i} - 1 - (\delta_i - 2\mu)(c_i + 2\delta_i\rho)/\delta_i}{2(\mu - \frac{\delta_i}{2})^2} \right] \\ &> E_\mu(T'_1) + o\left(\frac{p_1}{1 - p_1} E_\mu(T_1)\right) \end{aligned}$$

as $L \rightarrow \infty$ for $i \geq 2$. Hence, $\sum_{k=1}^m p_k E_\mu(T_k) > E_\mu(T'_1) \geq E_\mu(T_C^*)$ as $L \rightarrow \infty$ since $(1 + o(1))E_\mu(T_1) = E_\mu(T'_1)$. (ii). If $\delta_m > 2\mu, \delta_1 \leq 2\mu$ or $\delta_m = 2\mu, \delta_1 < 2\mu$, then $E_\mu(T_m)/E_\mu(T_1) \rightarrow +\infty$ as $L \rightarrow +\infty$. (iii). If $\delta_m < 2\mu$, then

$$E_\mu(T_k) = (1 + o(1)) \frac{2c_k}{\delta_k(2\mu - \delta_k)} > (1 + o(1)) \frac{2c_i}{\delta_i(2\mu - \delta_i)} = E_\mu(T_i)$$

for $k \neq i$, where the parameter δ_i satisfies $\delta_i(2\mu - \delta_i) = \max_{1 \leq k \leq m} \delta_k(2\mu - \delta_k)$. Thus, $\sum_{k=1}^m p_k E_\mu(T_k) > E_\mu(T'_i) \geq E_\mu(T_C^*)$ as $L \rightarrow \infty$. By (i), (ii) and (iii), (4.10) of Theorem 3 follows.

Let T_{OE} denote the optimal EWMA chart with the reference value $r^* = 2a^*\delta_1^2/b^2$ ($0 < r^* \leq 1$), where $a^* \approx 0.5117, b > 0$ is the control limit such that $E_0(T_{OE}) = L$. It has been shown by Wu (1994) and Srivastava and Wu (1997) that $E_\mu(T_E) \geq E_\mu(T_{OE})$ as $L \rightarrow \infty$, and

$$E_0(T_{OE}) \sim \frac{e^{0.834\delta_1} e^{b^2/2'}}{0.408\delta_1^2 b}, \tag{A.13}$$

$$E_{\mu}(T_{OE}) = \frac{1}{\delta_1^2} \left[\frac{-\ln(1 - \frac{\sqrt{a^*}\delta_1}{\mu})}{2a^*} (b - \varepsilon(b))^2 - \frac{\delta_1^2 (1 - (1 - \frac{\sqrt{a^*}\delta_1}{\mu})^2)}{4\mu^2 (1 - \frac{\sqrt{a^*}\delta_1}{\mu})^2} + o\left(\frac{1}{(b - \varepsilon(b))^2}\right) \right] \quad (\text{A.14})$$

for $\mu > \sqrt{a^*}\delta_1$, where $0 < \varepsilon(b) < D/b$ and D is a constant. We can further show that

$$E_{\mu}(T_{OE}) \geq \sqrt{2\pi}b \left(1 - \frac{\mu}{\sqrt{a^*}\delta_1}\right) \exp\left\{\frac{b^2}{2} \left(1 - \frac{\mu}{\sqrt{a^*}\delta_1}\right)^2\right\}$$

for $\mu < \sqrt{a^*}\delta_1$ and $E_{\mu}(T_{OE}) \geq 2\sqrt{2\pi}b^2\sqrt{\ln b}$ for $\mu = \sqrt{a^*}\delta_1$ as $L \rightarrow \infty$. Thus, to prove (4.11) of Theorem 3, we need only prove $E_{\mu}(T_{OE}) > E_{\mu}(T_C^*)$. Since $E_0(T_{OE}) = L = E_0(T_k)$, $1 \leq k \leq m$, it follows from (4.5) and (4.13) that $b^2 = 2c_1 + o(1)$. By $\mu > \delta_1/2$, we may assume $\mu \in I_k$, where $k \geq 1$. We have proved in the proof of Theorem 2 that

$$E_{\mu}(T_C^*) \sim E_{\mu}(T'_k) \sim \frac{c'_k}{\delta_k(\mu - \frac{\delta_k}{2})} \quad (\text{A.15})$$

as $L \rightarrow \infty$. Note that $\delta_k(\mu - \delta_k/2) \geq \delta_j(\mu - \delta_j/2)$ for $j \neq k$, and $c_i/c'_j \rightarrow 1$ as $L \rightarrow \infty$ for all $1 \leq i, j \leq m$. Thus we have $E_{\mu}(T_j) \geq E_{\mu}(T'_k)$ for $j \neq k$ and $E_{\mu}(T_k) \sim E_{\mu}(T'_k)$. On the other hand, we have $E_{\mu}(T_{OE}) > E_{\mu}(T_1)$ for $\mu > \sqrt{a^*}\delta_1$ since $b^2 = 2c_1 + o(1)$ and $(\delta_1^2)^{-1} - \ln(1 - \sqrt{a^*}\delta_1/\mu)/2a^* > (\delta_1(2\mu - \delta_1))^{-1}$ as $L \rightarrow \infty$. Thus, it follows from (A.14) and (A.15) that $E_{\mu}(T_{OE}) > E_{\mu}(T_C^*)$ as $L \rightarrow \infty$, proving (4.11) of Theorem 3.

References

- Brook, D. and Evans, D. A. (1972). An approach to the probability distribution of Cusum run length. *Biometrika* **59**, 539-549
- Capizzi, G. and Masarotto, G. (2003). An adaptive exponentially weighted moving average control chart. *Technometrics* **45**, 199-207.
- Dragalin, V. (1993). The optimality of generalized CUSUM procedure in quickest detection problem. Proceedings of Steklov Math. Inst.: *Statistics. and Control of Stochastic Processes* **202**, 132-148.
- Dragalin, V. (1997). The design and analysis of 2-CUSUM procedure. *Comm. Statist. Simulation Comput.* **26**, 67-81.
- Han, D. and Tsung, F. G. (2004). A generalized EWMA control chart and its comparison with the optimal EWMA, CUSUM and GLR schemes. *Ann. Statist.* **32**, 316-339.
- Hawkins, D. M. and Olwell, D. H. (1998). *Cumulative Sum Charts and Charting for Quality Improvement*. Springer-Verlag, New York.

- Lai, T. L. (1995). Sequential change-point detection in quality control and dynamic systems. *J. Roy. Statist. Soc. Ser. B* **57**, 613-658.
- Lorden, G. (1971). Procedures for reacting to a change in distribution. *Ann. Math. Statist.* **42**, 520-527.
- Lorden, G. and Eisenberger, I. (1973). Detection of Failure rate increases. *Technometrics* **15**, 167-175.
- Lucas, J. M. (1982). Combined Shewhart-CUSUM quality control scheme. *J. Quality Tech.* **14**, 51-59.
- Lucas, J. M. and Saccucci, M. S. (1990). Exponentially weighted moving average control schemes: properties and enhancements. *Technometrics* **32**, 1-16.
- Montgomery, D. C. (1996). *Introduction to Statistical Quality Control*. 3rd edition. Wiley, New York.
- Moustakides, G. V. (1986). Optimal stopping times for detecting changes in distribution. *Ann. Statist.* **14**, 1379-1387.
- Ritov, Y. (1990). Decision theoretic optimality of the cusum procedure. *Ann. Statist.* **18**, 1464-1469.
- Rowlands, J., Nix, B., Abdollahian, M. and Kemp, K. (1982). Snub-nosed V-Mask Control Schemes. *The Statistician* **31**, 1-10.
- Siegmund, D. (1985). *Sequential Analysis: Tests and Confidence Intervals*. Springer-Verlag, New York.
- Siegmund, D. and Venkatraman, E. S. (1995). Using the generalized likelihood ratio statistic for sequential detection of a change-point. *Ann. Statist.* **23**, 255-271.
- Sparks, R. S. (2000). CUSUM charts for signalling varying location shifts. *J. Quality Tech.* **32**, 157-171.
- Srivastava, M. S and Wu, Y. H. (1993). Comparison of EWMA, CUSUM and Shiryaev-Roberts procedures for detecting a shift in the mean. *Ann. Statist.* **21**, 645-670.
- Srivastava, M. S and Wu, Y. H. (1997). Evaluation of optimum weights and average run lengths in EWMA control schemes. *Comm. Statist. Theory Methods* **26**, 1253-1267.
- Wu, Y. H. (1994). Design of control charts for detecting the change. In *Change-point Problems*, **23** (Edited by E. Carlstein, H. Muller and D. Siegmund), 330-345. Inst. Math. Statist., Hayward, California.

Department of Mathematics, Shanghai Jiao Tong University, Shanghai 200030, P. R. China.

E-mail: donghan@sjtu.edu.cn

Department of Industrial Engineering and Engineering Management, Hong Kong University of Science and Technology, Kowloon, Hong Kong.

E-mail: season@ust.hk

Department of Mathematics, Xinjiang University, Xinjiang 830046, P. R. China.

E-mail: xijianhu@126.com

Department of Industrial Engineering and Engineering Management, Hong Kong University of Science and Technology, Kowloon, Hong Kong.

E-mail: kbwang@ust.hk

(Received February 2005; accepted January 2006)